Human Molecular Genetics, 2020, Vol. 29, No. R1 R108–R117

doi: 10.1093/hmg/ddaa133
Advance Access Publication Date: 27 June 2020
Invited Review Article

INVITED REVIEW ARTICLE

Temple syndrome and Kagami-Ogata syndrome: clinical presentations, genotypes, models and mechanisms

Rexxi Prasasya[1], Kristen V. Grotheer[2], Linda D. Siracusa[2] and Marisa S. Bartolomei[1,*]

[1]Epigenetics Institute, Department of Cell and Developmental Biology, Perelman School of Medicine, University of Pennsylvania, Philadelphia, PA 19104, USA and [2]Department of Medical Sciences, Hackensack Meridian School of Medicine at Seton Hall University, 340 Kingsland Street, Building 123, Nutley, NJ 07110, USA

*To whom correspondence should be addressed at: 9-122 Smilow Center for Translational Research, 3400 Civic Center Blvd., Philadelphia, PA 19104, USA. Tel: (215) 898-9063; Fax: (215) 898-9871; Email: bartolom@pennmedicine.upenn.edu

Abstract

Temple syndrome (TS) and Kagami-Ogata syndrome (KOS) are imprinting disorders caused by absence or overexpression of genes within a single imprinted cluster on human chromosome 14q32. TS most frequently arises from maternal UPD14 or epimutations/deletions on the paternal chromosome, whereas KOS most frequently arises from paternal UPD14 or epimutations/deletions on the maternal chromosome. In this review, we describe the clinical symptoms and genetic/epigenetic features of this imprinted region. The locus encompasses paternally expressed protein-coding genes (*DLK1, RTL1* and *DIO3*) and maternally expressed lncRNAs (*MEG3*/*GTL2*, *RTL1as* and *MEG8*), as well as numerous miRNAs and snoRNAs. Control of expression is complex, with three differentially methylated regions regulating germline, placental and tissue-specific transcription. The strong conserved synteny between mouse chromosome 12aF1 and human chromosome 14q32 has enabled the use of mouse models to elucidate imprinting mechanisms and decipher the contribution of genes to the symptoms of TS and KOS. In this review, we describe relevant mouse models and highlight their value to better inform treatment options for long-term management of TS and KOS patients.

Introduction

Genomic imprinting is a mammalian-specific phenomenon that results in the parental-specific expression of a small number of genes (1). Imprinted genes are generally found in clusters and regulated by imprinting control regions (ICRs), which exhibit parental-specific DNA methylation that is acquired during germline development. Critically, gamete-specific DNA methylation at ICRs is maintained after fertilization despite the large amount of epigenetic reprogramming that occurs at this time. This unique maintenance of DNA methylation can be explained by ICR-specific recognition of the Krüppel-associated box-containing zinc finger proteins (KZFP) ZFP57 and ZFP445 (2,3), as well the maintenance DNA methyltransferase DNMT1. Deletions or abnormal DNA methylation of ICRs results in perturbed imprinting of multiple genes in a cluster.

Much of what has been learned about imprinting in the past four decades is conserved between mouse and humans, enabling the use of both human genetics and mouse

Received: June 17, 2020. **Revised:** June 22, 2020. **Accepted:** June 24, 2020

models to elucidate genes and mechanisms. Though numbering only in the hundreds, imprinted genes can explain the block to complete uniparental development in mammals. Additionally, because imprinted genes are expressed from one parental allele, heterozygous mutations can result in abnormal phenotypes or even lethality. Further, given the central role for epigenetic gene regulation of imprinted genes, defects in DNA methylation, or epimutations, trigger abnormal expression and phenotypes. Consistently, human imprinting disorders have been described that result from heterozygous mutations, large or small deletions, uniparental disomy (UPD) and ICR epimutations (biallelic loss or gain of DNA methylation). Examples of human imprinting disorders include the growth disorders, Beckwith-Wiedemann syndrome (BWS) and Silver-Russell syndrome (SRS), and the neurobehavioral disorders Prader-Willi syndrome (PWS) and Angelman syndrome (AS) (4,5). Importantly, because of human and mouse imprinting conservation, mouse models have been instrumental to understanding mechanisms, genotype-phenotype correlations and pursuing therapeutic options (6,7).

Temple syndrome (TS: OMIM #616222; ORPHA: #254516) and Kagami-Ogata syndrome (KOS: OMIM #608149; ORPHA: #254534) are two additional genomic imprinting disorders that result from genetic and epigenetic alterations of a large imprinted gene cluster in the Chromosome 14q32 region. As with the imprinting disorders above, this region is conserved in mouse. TS was first described in individuals who exhibited short stature and premature puberty (8), whereas KOS was first described in individuals with multiple congenital anomalies (9). Although the initial cases were classified as maternal or paternal UPDs, respectively, and were considered rare (<1 in 1,000,000), there is growing realization that the disorders are more common and have a variety of etiologies. In some cases, molecular genetic and epigenetic testing is required to confirm a diagnosis, as patients with either KOS (10) or TS (11) have been misdiagnosed as having more common imprinting disorders such as PWS, AS, BWS or SRS.

This review is designed to (1) provide a clinical overview of symptoms and (2) describe the genetic and epigenetic alterations underlying TS and KOS, with the goal of appropriately identifying infants, children and adults with these disorders. Moreover, we describe how mouse models are used to provide insight into the mechanisms of imprinting and the contribution of genes in the region to phenotypes. Ultimately, the diagnosis of TS or KOS is essential for infants to receive appropriate medical treatment early in life and to provide families with expectations for their children's clinical course, recommendations for support services and appropriate counseling for recurrence risks.

Clinical Symptoms in TS

The common signs and symptoms of TS are shown in Table 1. The cardinal features of children with TS are low birth weight, feeding problems, hypotonia and motor delay, mild facial dysmorphism, short stature and premature puberty (OMIM #616222; ORPHA: #254516). Hypotonia is associated with poor feeding and limited suck reflex early in life (11–13). Low birth weight is due to intrauterine growth restriction (11–13). In some cases, these characteristics contribute to a formal diagnosis of failure to thrive (14–16).

Facial features range from mild to moderate dysmorphia and may not be evident in neonates, but become distinguishable with age. Frontal bossing and micrognathia are common in infants (11–13,17). Face shape may be long or triangular, due to prominent forehead and small jaw (12,15,18). Many patients have been described clinically with 'flat facial features' (11,12,15,17,18). Skeletal features that help with diagnosis include small hands and/or feet, disproportionate to the rest of the body, as well as clinodactyly and joint hypermobility (11–13,15,17,18). Growth hormone has been used as a treatment for short stature (11,13,19).

Development ranges from normal to severely delayed. Motor delay often presents with delay in walking (13,17,18). Children may experience speech delay and/or intellectual disability, and require special accommodations in school settings (11,12). Children with TS should be evaluated for developmental delays and provided with early intervention services.

Endocrine anomalies are prevalent, with truncal obesity developing as early as 4–6 years (11,12,18). Obesity has been associated with compulsive excessive eating habits as well as normal eating habits (12). Diabetes and hypercholesterolemia have been reported (12,20,21). Most TS patients experience precocious puberty (11–13) along with advanced bone age (11,17,18); treatment with gonadotropin-releasing hormone agonists can delay the early signs of puberty (22).

Clinical Symptoms in KOS

Common signs and symptoms of KOS are shown in Table 1. The cardinal features of KOS infants are small bell-shaped thorax, coat-hanger ribs and narrow chest wall, which lead to significant respiratory distress upon delivery (OMIM #608149; ORPHA: #254534). Neonates often require intubation and high level care in the neonatal intensive care unit, and are discharged with oxygen and respiratory monitoring systems (23,24). Abnormal formation of the thoracic cavity can complicate feeding and contribute to failure to thrive and postnatal growth failure in infancy (10,25). Some KOS infants are born with heart anomalies (26,27).

Neonates with KOS may present with abdominal wall defects (25,26). Omphalocele is most prevalent, often detected on ultrasound before delivery and requiring surgical repair after delivery (10). Diastasis recti is highly reported in neonates as well. Inguinal hernia often presents later in infancy or during childhood (10,26). Hepatoblastoma has been reported in three children with KOS and monitoring has been suggested, but no formal guidelines have been developed (10).

Individuals with KOS often exhibit mildly dysmorphic craniofacial features, which may include a depressed nasal bridge, frontal bossing and a prominent philtrum (10,27,28). Other noteworthy traits include short neck, short palpebral fissures, anteverted nares and micrognathia (10,26). As they develop, children with KOS may experience speech and/or motor delays (10). Some children have mild intellectual disability, while others have normal intellectual ability (10). Children with KOS should be closely monitored for signs of developmental delay and provided with early intervention services.

Clinical Symptoms During the Prenatal Period

While TS and KOS are often not diagnosed until birth, several nonspecific symptoms may indicate a fetus carries one of these genetic abnormalities. Both syndromes are associated with preterm labor and often require cesarean section for delivery (10,12). In TS, oligohydramnios and small placenta contribute to intrauterine growth restriction (12,18). TS babies are

Table 1. Clinical characteristics of Temple syndrome and Kagami-Ogata syndrome

Features	Temple syndrome	Kagami-Ogata syndrome
Prenatal	Oligohydramnios[a] Preterm delivery[a] Intrauterine growth restriction/small for gestational age (SGA)[a] Small placenta Reduced fetal movement Delivery requiring cesarean section	Polyhydramnios[a] Preterm delivery[a] Omphalocele[a] Placentomegaly[a] Macrosomia[a] Delivery requiring cesarean section
Perinatal/Postnatal	Low birth weight and length[a] Feeding problems[a] Postnatal short stature[a]	Respiratory distress[a] Feeding problems[a] Postnatal growth retardation
Developmental/Neurological	Hypotonia[a] Motor delay[a] Speech delay[a] Global developmental delay[a] Intellectual disability[a]	Hypotonia[a] Speech delay[a] Motor delay[a] Mild intellectual disability
Craniofacial	Abnormal head circumference[a] Trigonocephaly[a] Depressed nasal bridge[a] Broad nose[a] Short philtrum[a] Micrognathia[a] Epicanthus Anteverted nares High-arched palate	Frontal bossing[a] Depressed nasal bridge[a] Anteverted nares[a] Prominent philtrum[a] Full cheeks[a] Micrognathia[a] Short neck[a] Hairy forehead
Thoracic	Uncommon	Small bell-shaped thorax[a] Coat-hanger ribs[a] Narrow chest wall[a] Heart anomaly
Abdominal	Uncommon	Omphalocele[a] Diastasis recti[a] Inguinal hernia
Musculo-skeletal	Small hands and/or feet[a] Clinodactyly[a] Joint hypermobility[a] Body asymmetry Kyphoscoliosis	Joint contractures[a] Kyphoscoliosis
Endocrine	Obesity[a] Early onset puberty[a] Advanced bone age Hypercholesterolemia Type II diabetes	Uncommon

Features listed from most common to least common in each category; [a]denotes a very common feature. Symptoms above were noted in 5 or more patients with TS or KOS. References are listed in Supplementary Material, Supplementary File #1; articles with patient photographs are indicated.

almost always small for gestational age (SGA) (11–13). Occasionally, reduced fetal movement may be detected on ultrasound during pregnancy (11,18). In KOS, polyhydramnios is a cardinal feature, often causing dyspnea in pregnant women and requiring amnioreduction (10,26). Omphaloceles are commonly detected on ultrasound, necessitating cesarean delivery and surgical repair (10). In contrast to babies with TS, KOS newborns often exhibit macrosomia (10,28).

Structure and Genes of the Chr 14q32 Imprinted Region

The imprinted region responsible for TS and KOS is shown in Figure 1. The centromeric end is proximal to the *DLK1* gene and the telomeric end is distal to the *DIO3* gene. The locus contains three differentially methylated regions (IG-DMR, MEG3-DMR, MEG8-DMR) (29–31). Protein-coding genes (*DLK1*, *RTL1*, *DIO3*), long ncRNAs (*MEG3*, *MEG8*, *RTL1as*, *DIO3OS*) and short ncRNAs (*SNORDs* and *miRNAs*) are transcribed based on parent-of-origin (Table 2). TS and KOS are most commonly caused by UPD followed by epimutations and deletions (Fig. 1). Rare cases involve inherited or *de novo* Robertsonian translocations (15,24) or mosaicism (32–34).

Genetic and Epigenetic Testing

A diagnosis of TS or KOS based on clinical characteristics alone may sometimes be difficult, especially if symptoms are mild. The rarity of these disorders along with features that resemble those in more common imprinting syndromes may contribute to misdiagnosis. For example, TS can be considered an undergrowth disorder, with some features (e.g. SGA, short stature,

Table 2. Genes in the Human Chr 14q32 and Mouse Chr 12 imprinted regions

Human symbol[a]	Human gene name	Mouse symbol	Expression	Function	References
DIO3	Deiodinase, Iodothyronine Type III	*Dio3*	High biallelic expression in placenta and pregnant uterus; high expression in fetus, fetal liver, testis, bladder; preferential paternal expression in neonatal foreskin; preferential maternal expression in adult skin; region-specific preferential maternal expression of a larger *DIO3* transcript in brain, similar to *DIO3OS*	Maintains low serum T3 concentrations in placenta; the DIO3 selenoenzyme catalyzes the conversion of T4 and T3 to the inactive metabolites rT3 and T2, respectively; may prevent premature exposure of developing fetal tissues to adult levels of thyroid hormones; regulates circulating fetal thyroid hormone concentrations; dysregulation may contribute to neurological symptoms	Hernandez *et al.* (74); Martinez *et al.* (77); Hernandez and Stohn (78)
DIO3OS (DIO3-AS1)	Deiodinase, Iodothyronine Type III, Opposite Strand	*Dio3os (Dio3as)*	LncRNA with 12 isoforms; expressed in most tissues with highest expression in testis, adrenal cortex, prostate, bladder, uterus, placenta, and fetal lung; region-specific imprinted expression in brain, similar to *DIO3*	Suggested role in maintaining paternal-only expression of *DIO3*; the 5′ end of two *DIO3OS* transcripts encode *hsa-mir-1247*	Hernandez *et al.* (74)
DLK1 (PREF1)	Delta-like non-canonical notch ligand 1	*Dlk1*	Paternal expression in fetus, hypothalamus, preadipocytes	An epidermal growth factor repeat-containing transmembrane protein; the protein is cleaved by TACE to generate an active soluble form; soluble DLK1 interacts with FN1 to activate integrin downstream MEK/ERK signaling, upregulate SOX9, and inhibit adipocyte differentiation; loss of DLK1 results in precocious puberty and increased adiposity	Dauber *et al.* (69,85)
MEG3 (GTL2)	Maternally expressed gene 3	*Meg3 (Gtl2)*	LncRNA—maternal expression with multiple transcripts; highly expressed in brain and pituitary	Unclear in humans; potential role in angiogenesis, brain development and function, and tumorigenesis from mouse studies	Gordon *et al.* (79)
MEG8	Maternally expressed gene 8	*Rian (Meg8)*	LncRNA—maternal expression with multiple transcripts that include the *SNORDs*; highly expressed in brain, uterus, and heart	Unknown	Charlier *et al.* (80)
RTL1 (PEG11)	Retrotransposon-like gene 1	*Rtl1*	Highly expressed protein at the late fetal stage in fetus and placenta; expression is 5-fold higher in the absence of *RTL1as*	Essential for normal development of placenta and fetus; maintenance of capillaries in the fetus	Ito *et al.* (67)
RTL1as (anti-PEG11)	Retrotransposon-like gene 1 antisense	*Rtl1as*	LncRNA encoding *miRNAs* – *431*, *–433*, *–127*, *–432*, and – *136*	Contains miRNAs targeting the *RTL1* transcript *in trans* through an RNA interference (RNAi) mechanism	Seitz *et al.* (45); Davis *et al.* (81)
miRNAs (hsa-mir-#)	microRNAs	*Mirg and miRNAs (Meg9)*	Maternal expression of *miRNA-154*, *miRNA-379*, *miRNA-544*, *miRNA-654* family members and other *miRNAs*; expressed throughout human vasculature	Translational repression and/or gene silencing of target mRNAs; potential role in vascular remodeling and Type II Diabetes; summary of individual miRNA's involvement in disease pathogenesis in Benetatos et al. 2013 (73)	Benetatos *et al.* (73); Goossens *et al.* (82); Kameswaran *et al.* (83)
SNORDs (orphan *snoRNAs*)	C/D box small nucleolar RNAs	*Snord(s)*	Multiple tandem copies of *SNORD-112*, *–113*, *–114 are* highly expressed ncRNAs from maternal chromosome; differential expression in brain and throughout human vasculature	General role in posttranslational rRNA modification, pre-mRNA splicing, and polyadenylation of genes; Chr 14q32 *SNORDs* direct 2'O-ribose-methylation via Fibrillarin of non-canonical RNA targets; potential roles in vascular remodeling and cardiovascular disease	Hakansson *et al.* (84)

[a]Previous gene symbols are shown in () below the current gene symbol.

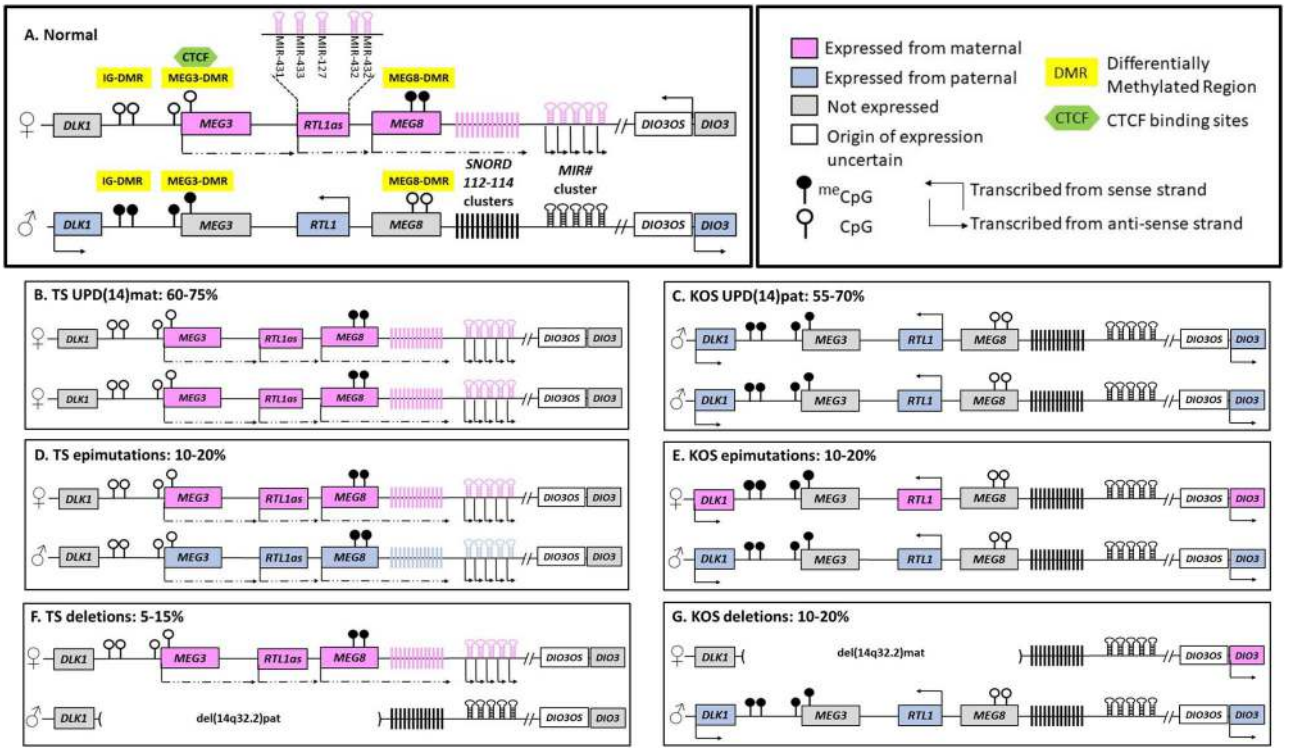

Figure 1. Genetic and epigenetic alterations on Chromosome 14 lead to Temple syndrome or Kagami-Ogata syndrome. The human Chr 14q32 region extending from 100.7 to 101.6 Mb is shown (Ensembl: Human GRCh38.p13). Hashmarks (//) indicate the largest interval of 513 kb which lies between the 3′ end of the *MEG8* gene and the 3′ end of the *DIO3OS* gene. The methylation pattern of the IG-DMR is established in the germline (29). The *MEG3*-DMR lies in the promoter region of the *MEG3* gene; its methylation pattern is set postfertilization and is dependent on the methylation pattern of the IG-DMR (30). The *MEG8*-DMR lies in intron 2 of the *MEG8* gene (72). Methylation of the *MEG8*-DMR occurs at or after week 17 of fetal development and may be dependent on the IG-DMR and/or *MEG3*-DMR (31), as well as transcription starting at the upstream *MEG3* promoter and extending through the *MEG8*-DMR (11). Most postnatal tissues show differential methylation of the *MEG8*-DMR, consistent with imprinting (11). The *MEG3*, *RTL1as*, *MEG8* and *SNORD* genes may be transcribed as polycistronic transcripts (65,73). The CpG-rich 1.2 kb promoter of the *DIO3OS* and *DIO3* genes lies between them, although additional promoters outside this region have been suggested (74). Although the direction of transcription of *DIO3OS* is known (74), the parental origin of transcription in humans is unknown. Alterations leading to TS and KOS are diagrammed in the left and right columns, respectively. The % represents an estimate of the frequency of cases that are due either to UPD, epimutations or deletions, based on reports describing multiple cases (11,12,22,65,75). (**A**) Normal imprinting, methylation and gene expression at the Chr 14q32 region. The imprinted region begins proximal to the *DLK1* gene and ends distal to the *DIO3* gene. (**B**) TS can be caused by maternal UPD leading to expression of only maternally expressed genes from both chromosomes, whereas (**C**) KOS can be caused by paternal UPD leading to expression of only paternally expressed genes from both chromosomes. UPD may be segmental or involve the whole chromosome. (**D**) TS may be caused by hypomethylation of the IG-DMR and *MEG3*-DMR on the paternal chromosome, leading to a maternal chromosome-like expression pattern. (**E**) Conversely, KOS may be caused by hypermethylation of the IG-DMR and *MEG3*-DMR on the maternal chromosome, leading to a paternal chromosome-like expression pattern. (**F**) TS may be caused by deletions in the paternally inherited chromosome, leading to absence of paternally expressed genes, (**G**) whereas KOS may be caused by deletions in the maternal chromosome, leading to absence of maternally expressed genes. Microdeletions involving the IG-DMR and/or the *MEG3*-DMR may also cause TS or KOS. Not drawn to scale.

hypotonia and speech delay) resembling those found in PWS or SRS (11,22). Although a hallmark feature of TS is precocious puberty, this diagnosis cannot be made in infants. Similarly, KOS can be considered a disorder of overgrowth, with some prenatal features (e.g. placentomegaly, omphalocele and fetal macrosomia) resembling those found in BWS (10,27).

Genetic and epigenetic platforms that could collectively analyze and distinguish among genomic imprinting disorders (such as PWS, AS, BWS, SRS and now TS and KOS) are needed to aid clinical diagnoses. Although single nucleotide polymorphism microarrays detect isodisomy and large deletions; next-generation sequencing can define deletion breakpoints and other alterations. Platforms to assess the entire methylome exist, but regional analysis of DNA methylation status must be ordered individually for each locus using methylation-specific (MS) multiplex ligation-dependent probe amplification (MS-MLPA) or MS-PCR (35). Recently, a DNA methylation platform was specifically designed to detect multiple methylation abnormalities across a set of imprinting conditions and genes (EpiSign Complete) (36,37). These assays can confirm a clinical diagnosis as well as detail the genetic/epigenetic anomalies that underlie individual cases of TS and KOS. This determination is necessary to appropriately counsel families regarding recurrence risk. Although mosaicism has been reported in only a few cases of TS and KOS (32–34), the true number of mosaic individuals may be underestimated. Current tests have a high sensitivity to detect mosaicism, especially if multiple tissues are evaluated, as demonstrated in related imprinting disorders, such as BWS (38,39).

Imprinting at mouse distal chromosome 12

Imprinted genes at mouse chromosome 12aF1 were first suggested when embryonic lethality was observed for both maternal and paternal disomies or duplications of the distal portion of chromosome 12 in historical genetic studies using Robertsonian or reciprocal translocation heterozygote intercrosses (40). Indeed, this region contains the ~1 Mb *Dlk1-Dio3* imprinted region syntenic with human chromosome 14 where TS and KOS map (41–48).

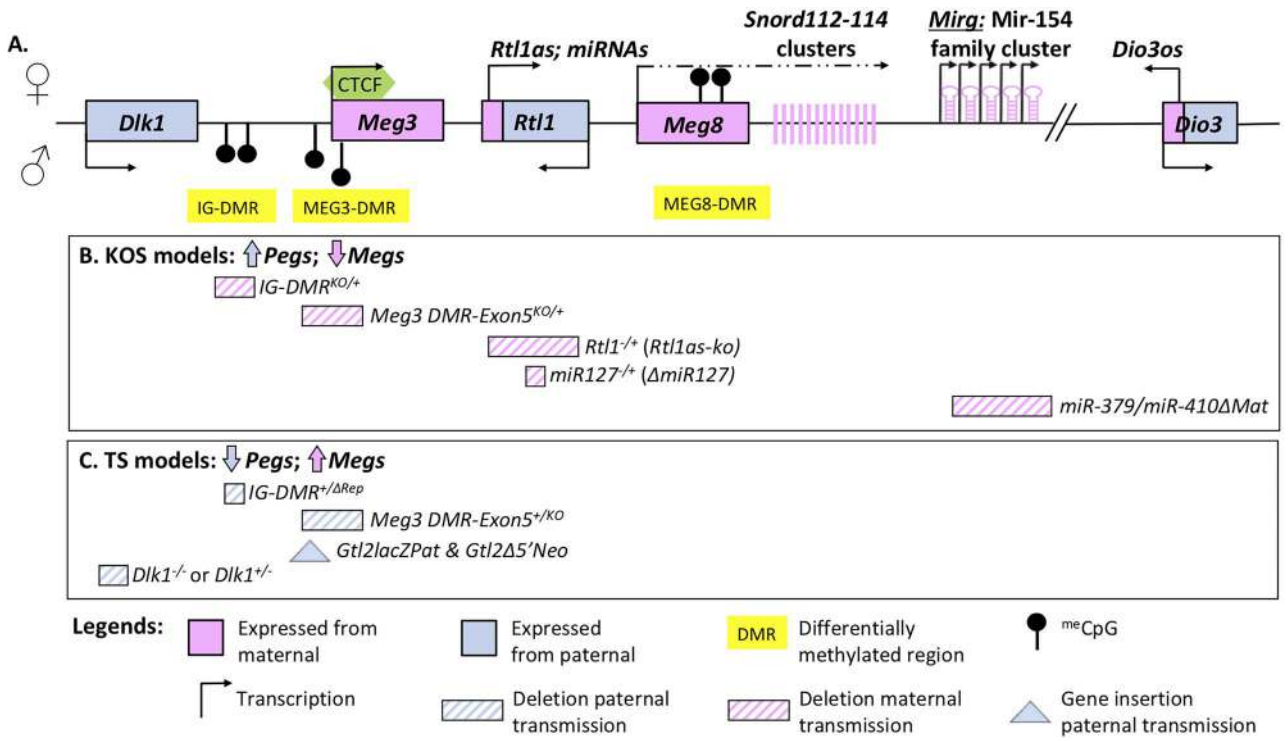

Figure 2. Mouse *Dlk1-Dio3* Imprinted locus. (**A**) Located in the distal portion of chromosome 12, the mouse *Dlk1-Dio3* spans ~1 Mb and shares similar regulatory mechanisms as the human *DLK1-DIO3* locus (detailed in Fig. 1). The germline ICR, *IG-DMR*, is located ~15 Kb upstream of *Meg3* and 70 Kb downstream of *Dlk1*. In mouse embryonic stem cells, CTCF binding to the unmethylated *Meg3-DMR* is important for monoallelic expression of *Dlk1* (76). (**B** and **C**) Summary of KOS and TS mouse models described in this review. Gene deletions or insertions are aligned to the native locus illustrated above in (A). Striped boxes indicate gene deletions, while a filled triangle indicates gene insertion. Color filling designates the parental inheritance of the mutated allele.

The largely conserved regulatory mechanisms within the *Dlk1-Dio3* locus between mouse and human (see Figs 1 and 2A) (49) substantiate the use of genetic mouse models to explore the molecular basis for KOS and TS. The characteristic bell-shaped thorax, abdominal wall defects and placentomegaly characteristic of KOS is recapitulated in several mouse models with loss of maternally expressed genes (*Megs*) or overexpression of paternally expressed genes (*Pegs*). In contrast, while several mouse models with overexpression of *Megs* or loss of *Pegs* display the growth restriction and hypotonia observed in TS, these perturbations to the *Dlk1-Dio3* locus do not cause the precocious puberty prevalent in TS patients. Subsequent discussion will focus on relating changes in gene expression within the locus to the phenotypes observed in these mouse models (summarized in Fig. 2B and C).

Uniparental disomies of mouse chromosome 12

Paternal UPD of chromosome 12—*PatUpd(12)*—is 50% lethal by late gestation (E18.5) (50,51). In addition to recapitulating the skeletal and placental abnormalities of KOS, *PatUpd(12)* causes a mouse-specific phenotype of enlarged myofibers comprised of cells with centrally located nuclei resembling immature myotubules (50). Duplication of the paternal distal chromosome 12—*PatDp(dist12)*—phenocopies the whole chromosome duplication with increased severity of lethality by E16.5, implicating distal chromosome 12 as the location of the imprinted loci (52).

In agreement with human MatUPD(14) and TS, maternal UPD of chromosome 12—*MatUpd(12)*—is associated with a less severe phenotype than *PatUpd(12)* as pups can survive to term, but die perinatally due to severe respiratory distress (50). The consequence of overexpression of the maternally expressed non-coding transcripts within the *Dlk1-Dio3* locus was further clarified using transgenic overexpression of *Meg3* (also called *Gtl2*), *Rtl1as* and *Meg8* (*Meg3-Meg8 MatTg*), which recapitulate the growth restriction and perinatal lethality observed in *MatUpd(12)* pups (53). In this model, expression of several downstream growth promoting genes are suppressed during embryonic development, suggesting that maternally expressed non-coding transcripts govern expression of growth regulators (53).

Deletions targeting *IG-DMR*

The germline ICR for the *Dlk1-Dio3* locus is an 8 kb intergenic CpG island that is methylated on the paternal allele (Fig. 2) (44). Maternal transmission of *IG-DMR* deletion (*IG-DMR*$^{KO/+}$) leads to embryonic lethality by E16.5 and KOS-like phenotypes in the embryo (54). This deletion causes locus-wide loss of imprinting (LOI), including biallelic *Dlk1* expression, overexpression of *Rtl1* (4.5x), and *Dio3* (2x), hypermethylation of the *Meg3-DMR* and silencing of downstream *Megs* expression (54,55). Placental defects are not observed in *IG-DMR*$^{KO/+}$ as explained by a less severe LOI in the *IG-DMR*$^{KO/+}$ placenta, downregulated expression of *Megs* and only modest upregulation of *Dlk1, Rtl1* and *Dio3* (54). This result suggests non-conserved placenta-specific imprinting regulation for the *Dlk1-Dio3* locus. In contrast to the maternal deletion, paternal deletion of the methylated *IG-DMR* (*IG-DMR*$^{+/KO}$) is viable and exhibits no gene expression changes (55).

As described above, methylation at ICRs requires protection during postfertilization genome wide reprogramming (2,3). Recently, a model was developed to investigate the function of

a tandem repeat array within the mouse *IG-DMR* (*IG-DMR*$^{+/\Delta Rep}$) (56). Paternal transmission of the tandem repeat deletion caused postfertilization loss of *IG-DMR* methylation, approximating a type of epimutation that is observed in TS cases (16,56–58). In this model, the paternal *Meg3-DMR* never acquired methylation, resulting in biallelic expression of maternal transcripts and the loss of *Pegs* expression (56). Both *IG-DMR*$^{+/\Delta Rep}$ embryo and placenta become severely growth restricted beginning at E13.5, with pups dying shortly after birth. These results suggest that ZFP57 or ZFP445 binding motifs with the tandem repeats are required for ICR methylation protection (2,3,49,56).

Meg3-DMR and promoter mutations

The 5′ end of *Meg3* gains methylation on the paternal allele proximal to implantation (E6.5) (59). Maternal deletion of the *Meg3-DMR* (*Meg3DMR-Exon5*$^{KO/+}$) eliminates the functional *Meg3* promoter and is accompanied by decreased expression of *Rtl1as, Meg8* (*Rian*) and *miRNAs* from the *Mirg* clusters (60,61). Two independent lines of *Meg3DMR-Exon5*$^{KO/+}$ were developed, with the mutant described by Zhou and colleagues resulting in overexpression of *Pegs* (60,61). Regardless of the expression status of *Pegs*, neither knockout line develops KOS-like skeletal defects. Instead, perinatal lethality occurred in both models due to severe hypoplastic pulmonary alveoli and diaphragm muscle defects (60,61).

Paternal deletion of the *Meg3-DMR* activates downstream *Megs* expression from the normally silenced paternal allele and loss of expression of *Dlk1, Rtl1 and Dio3* (60). These molecular phenotypes are also observed following gene insertion immediately upstream of the paternal *Meg3*-DMR, which is associated with hypomethylation of the DMR (*Gtl2lacZPat, Gtl2Δ5'NeoPat*) (62,63). These mutations cause severe growth restriction that is consistent with TS and the majority of mutant pups die neonatally. Proportional dwarfism remains in offspring that survive to adulthood, although precocious puberty is not observed in fertile adult mutants (60,63). Additional characterization of *Gtl2lacZPat* mutants shows disruption to the insulin-like growth factor-1 (Igf-1) signaling pathway and compromised glucose tolerance in the surviving animals (64). This finding may inform the underlying cause of endocrine and metabolic phenotypes observed in a subset of TS cases (11,12,18).

Single gene knockouts within the *Dlk1-Dio3* locus

Because UPDs and large deletions or epimutations often cause misexpression of multiple genes in the KOS/TS critical region, it has been difficult to attribute phenotypes to specific genes. Single gene mutations, however, have provided more insight. A candidate etiology for KOS embryonic and placental phenotypes is the overexpression of *RTL1* (65). In both mouse and human, miRNAs processed from the maternally expressed *Rtl1as* antagonize *Rtl1* transcripts through an RNA interference mechanism (45). Maternal deletion of *Rtl1as* (*Rtl1as-ko*) (66) or *miR-127* (*ΔmiR127*) (67) results in functional overexpression of *Rtl1*. Both deletions lead to placentomegaly with dilated fetal capillaries beginning at E16.5, consistent with KOS placentas. In contrast, embryos are unaffected by *Rtl1* overexpression because pups develop normally (45,66), suggesting that Rtl1 protein is likely to be the most functional in the placenta.

Maternal deletion of *miR-379/410* (*miR-379/mir-410ΔMat*) from the *Mirg* clusters causes poor neonatal survival due to inefficient activation of gluconeogenesis in the term fetus, a process that is required to survive parturition (68). This finding may better inform the developmental delay and feeding difficulties observed in a subset of KOS neonates (65).

In human, loss of function of the paternally expressed *DLK1* gene is associated with familial cases of central precocious puberty, often unaccompanied by growth restriction that is characteristic of TS (69,70). In mouse, *Dlk1* knockout (*Dlk1*$^{-/-}$, *Dlk1*$^{+/-}$) causes severe embryonic and postnatal growth retardation, typically resulting in perinatal death (71). Of *Dlk1*$^{-/-}$ mice that survived to adulthood, no central precocious puberty was observed. Rather, *Dlk1*$^{-/-}$ mice displayed metabolic phenotypes of hypercholesterolemia, hyperlipidemia and fatty liver disease when challenged on high fat diet, a feature reported in 10–20% of TS cases (12,22).

Conclusions

TS and KOS are complex imprinting disorders that largely manifest in physical defects necessitating obligatory supportive therapies early in the life of affected individuals. Improved understanding of the molecular mechanisms regulating the *DLK1-DIO3* imprinted gene cluster have aided in the clinical diagnosis of TS and KOS, particularly in their differentiation from more common imprinting disorders. Clinical phenotypes associated with TS and KOS likely arise from complex interactions of multiple aberrantly expressed genes within the *Dlk1-Dio3* cluster, as evidenced from the various single gene knockout or overexpression models that cannot precisely recapitulate TS (e.g. precocious puberty) or KOS (e.g. skeletal defects) phenotypes.

Importantly, alterations in gene-dosage within the *Dlk1-Dio3* locus affect very early developmental processes including placentation, thus impacting fetal growth and musculoskeletal formation. Identification of targets of maternally expressed non-coding transcripts in this locus should be considered a priority for understanding TS and KOS. Emerging evidence shows that these non-coding transcripts can orchestrate expression of developmental growth regulators (53). Moving forward, knowledge gained from mouse models described here may inform treatment options for long-term management of TS and KOS patients through identification of druggable signaling pathways that are altered due to genetic and epigenetic mutations at the locus.

Supplementary Material

Supplementary Material is available at *HMG* Online.

Acknowledgements

We thank Dr Jennifer Kalish and Dr Helio Pedro manuscript review. The authors acknowledge the astute observations and significant contributions of Dr Karen Temple, Dr Masayo Kagami, Dr Tsutomu Ogata and Dr Jin-Chen Wang, which led to the identification of TS and KOS as distinct genomic imprinting disorders.

Conflict of Interest statement. None declared.

References

1. Barlow, D.P. and Bartolomei, M.S. (2014) Genomic imprinting in mammals. *Cold Spring Harb. Perspect. Biol.*, **6**, a018382.

2. Takahashi, N., Gray, D., Strogantsev, R., Noon, A., Delahaye, C., Skarnes, W.C., Tate, P.H. and Ferguson-Smith, A.C. (2015) ZFP57 and the targeted maintenance of Postfertilization genomic imprints. *Cold Spring Harb. Symp. Quant. Biol.*, **80**, 177–187.
3. Takahashi, N., Coluccio, A., Thorball, C.W., Planet, E., Shi, H., Offner, S., Turelli, P., Imbeault, M., Ferguson-Smith, A.C. and Trono, D. (2019) ZNF445 is a primary regulator of genomic imprinting. *Genes Dev.*, **33**, 49–54.
4. Kalish, J.M., Jiang, C. and Bartolomei, M.S. (2014) Epigenetics and imprinting in human disease. *Int. J. Dev. Biol.*, **58**, 291–298.
5. Nicholls, R.D. and Knepper, J.L. (2001) Genome organization, function, and imprinting in Prader-Willi and Angelman syndromes. *Annu. Rev. Genomics Hum. Genet.*, **2**, 153–175.
6. Chang, S. and Bartolomei, M.S. (2020) Modeling human epigenetic disorders in mice: Beckwith-Wiedemann syndrome and silver-Russell syndrome. *Dis. Model. Mech.*, **13**, dmm044123.
7. Resnick, J.L., Nicholls, R.D. and Wevrick, R. (2013) Recommendations for the investigation of animal models of Prader–Willi syndrome. *Mamm. Genome*, **24**, 165–178.
8. Temple, I.K., Cockwell, A., Hassold, T., Pettay, D. and Jacobs, P. (1991) Maternal uniparental disomy for chromosome 14. *J. Med. Genet.*, **28**, 511–514.
9. Wang, J.C., Passage, M.B., Yen, P.H., Shapiro, L.J. and Mohandas, T.K. (1991) Uniparental heterodisomy for chromosome 14 in a phenotypically abnormal familial balanced 13/14 Robertsonian translocation carrier. *Am. J. Hum. Genet.*, **48**, 1069–1074.
10. Kagami, M., Kurosawa, K., Miyazaki, O., Ishino, F., Matsuoka, K. and Ogata, T. (2015) Comprehensive clinical studies in 34 patients with molecularly defined UPD(14)pat and related conditions (Kagami–Ogata syndrome). *Eur. J. Hum. Genet.*, **23**, 1488–1498.
11. Beygo, J., Küchler, A., Gillessen-Kaesbach, G., Albrecht, B., Eckle, J., Eggermann, T., Gellhaus, A., Kanber, D., Kordaß, U., Lüdecke, H.-J. *et al.* (2017) New insights into the imprinted MEG8-DMR in 14q32 and clinical and molecular description of novel patients with Temple syndrome. *Eur. J. Hum. Genet.*, **25**, 935–945.
12. Kagami, M., Nagasaki, K., Kosaki, R., Horikawa, R., Naiki, Y., Saitoh, S., Tajima, T., Yorifuji, T., Numakura, C., Mizuno, S. *et al.* (2017) Temple syndrome: comprehensive molecular and clinical findings in 32 Japanese patients. *Genet. Med.*, **19**, 1356–1366.
13. Brightman, D.S., Lokulo-Sodipe, O., Searle, B.A., Mackay, D.J.G., Davies, J.H., Temple, I.K. and Dauber, A. (2018) Growth hormone improves short-term growth in patients with Temple syndrome. *Horm. Res. Paediatr.*, **90**, 407–413.
14. Shin, E., Cho, E. and Lee, C.G. (2016) Temple syndrome: a patient with maternal hetero-UPD14, mixed iso- and heterodisomy detected by SNP microarray typing of patient-father duos. *Brain and Development*, **38**, 669–673.
15. Bertini, V., Fogli, A., Bruno, R., Azzarà, A., Michelucci, A., Mattina, T., Bertelloni, S. and Valetto, A. (2017) Maternal uniparental Disomy 14 (Temple syndrome) as a result of a Robertsonian translocation. *Mol. Syndromol.*, **8**, 131–138.
16. Kagami, M., Yanagisawa, A., Ota, M., Matsuoka, K., Nakamura, A., Matsubara, K., Nakabayashi, K., Takada, S., Fukami, M. and Ogata, T. (2019) Temple syndrome in a patient with variably methylated CpGs at the primary MEG3/DLK1: IG-DMR and severely hypomethylated CpGs at the secondary MEG3: TSS-DMR. *Clin. Epigenetics*, **11**, 42.
17. Lande, A., Kroken, M., Rabben, K. and Retterstøl, L. (2018) Temple syndrome as a differential diagnosis to Prader-Willi syndrome: identifying three new patients. *Am. J. Med. Genet. A*, **176**, 175–180.
18. Gillessen-Kaesbach, G., Albrecht, B., Eggermann, T., Elbracht, M., Mitter, D., Morlot, S., van Ravenswaaij-Arts, Schulz, S., Strobl-Wildemann, G., Buiting, K. *et al.* (2018) Molecular and clinical studies in 8 patients with Temple syndrome. *Clin. Genet.*, **93**, 1179–1188.
19. Stalman, S.E., Kamp, G.A., Hendriks, Y.M.C., Hennekam, R.C.M. and Rotteveel, J. (2015) Positive effect of growth hormone treatment in maternal uniparental disomy chromosome 14. *Clin. Endocrinol.*, **83**, 671–676.
20. Balbeur, S., Grisart, B., Parmentier, B., Sartenaer, D., Leonard, P.-E., Ullmann, U., Boulanger, S., Leroy, L., Ngendahayo, P., Lungu-Silviu, C. *et al.* (2016) Trisomy rescue mechanism: the case of concomitant mosaic trisomy 14 and maternal uniparental disomy 14 in a 15-year-old girl. *Clin. Case Rep.*, **4**, 265.
21. Chan, A.P., Mulatinho, M., Iskander, P., Lee, H., Martinez-Agosto, J.A. and Yeh, J. (2019) Maternal uniparental Disomy 14 (UPD14) identified by clinical exome sequencing in an adolescent with diverticulosis. *ACG Case Rep. J.*, **6**, 1–3.
22. Ioannides, Y., Lokulo-Sodipe, K., Mackay, D.J.G., Davies, J.H. and Temple, I.K. (2014) Temple syndrome: improving the recognition of an underdiagnosed chromosome 14 imprinting disorder: an analysis of 51 published cases. *J. Med. Genet.*, **51**, 495–501.
23. Huang, H., Mikami, Y., Shigematsu, K., Uemura, N., Shinsaka, M., Iwatani, A., Miyake, F., Kabe, K., Takai, Y., Saitoh, M. *et al.* (2019) Kagami-Ogata syndrome in a fetus presenting with polyhydramnios, malformations, and preterm delivery: a case report. *J. Med. Case Rep.*, **13**, 340.
24. Wang, X., Pang, H., Shah, B.A., Gu, H., Zhang, L., Wang, H. *et al.* (2020) A male case of Kagami-Ogata syndrome caused by paternal Unipaternal Disomy 14 as a result of a Robertsonian translocation. *Front. Pediatr.*, **8**, 88.
25. van der Werf, I.M., Buiting, K., Czeschik, C., Reyniers, E., Vandeweyer, G., Vanhaesebrouck, P., Lüdecke, H.-J., Wieczorek, D., Horsthemke, B., Mortier, G. *et al.* (2016) Novel microdeletions on chromosome 14q32.2 suggest a potential role for noncoding RNAs in Kagami-Ogata syndrome. *Eur. J. Hum. Genet.*, **24**, 1724–1729.
26. Luk, H.-M. (2017) Familial Kagami-Ogata syndrome in Chinese. *Clin. Dysmorphol.*, **26**, 124–127.
27. Altmann, J., Horn, D., Korinth, D., Eggermann, T., Henrich, W. and Verlohren, S. (2020) Kagami-Ogata syndrome: an important differential diagnosis to Beckwith-Wiedemann syndrome. *J. Clin. Ultrasound*, **48**, 240–243.
28. Yamamoto, Y. and Yoshida, K. (2019) EP15.11: two cases of Kagami-Ogata syndrome with congenital diastasis recti. *Ultrasound Obstet. Gynecol.*, **54**, 319–319.
29. Geuns, E., De Temmerman, N., Hilven, P., Van Steirteghem, Liebaers, I. and De Rycke (2007) Methylation analysis of the intergenic differentially methylated region of DLK1-GTL2 in human. *Eur. J. Hum. Genet.*, **15**, 352–361.
30. Kagami, M., O'Sullivan, M.J., Green, A.J., Watabe, Y., Arisaka, O., Masawa, N., Matsuoka, K., Fukami, M., Matsubara, K., Kato, F. *et al.* (2010) The IG-DMR and the MEG3-DMR at human chromosome 14q32.2: hierarchical interaction and distinct functional properties as imprinting control centers. *PLoS Genet.*, **6**, e1000992.

31. Bens, S., Kolarova, J., Gillessen-Kaesbach, G., Buiting, K., Beygo, J., Caliebe, A., Ammerpohl, O., Siebert, R. *et al.* (2015) The differentially methylated region of MEG8 is hypermethylated in patients with Temple syndrome. *Epigenomics*, **7**, 1089–1097.
32. Suzumori, N., Kagami, M., Kumagai, K., Goto, S., Matsubara, K., Sano, S. and Sugiura-Ogasawara, M. (2015) Clinical and molecular findings in a patient with 46,XX/47,XX, +14 mosaicism caused by postzygotic duplication of a paternally derived chromosome 14. *Am. J. Med. Genet. A*, **167**, 2474–2477.
33. Haug, M.G., Brendehaug, A., Houge, G., Kagami, M. and Ogat, T. (2018) Mosaic upd(14)pat in a patient with mild features of Kagami–Ogata syndrome. *Clin. Case Rep.*, **6**, 91.
34. Yakoreva, M., Kahre, T., Pajusalu, S., Ilisson, P., Žilina, O., Tillmann, V., Reimand, T. and Õunap, K. (2018) A new case of a rare combination of Temple syndrome and mosaic trisomy 14 and a literature review. *Mol. Syndromol.*, **9**, 182–189.
35. Cerrato, F., Sparago, A., Ariani, F., Brugnoletti, F., Calzari, L., Coppedè, F., De Luca, Gervasini, C., Giardina, E., Gurrieri, F., Nigro, C.L. *et al.* (2020) DNA methylation in the diagnosis of monogenic diseases. *Genes*, **11**, 355.
36. Aref-Eshghi, E., Kerkhof, J., Pedro, V.P., DI France, G., Barat-Houari, M., Ruiz-Pallares, N., Andrau, J.C., Lacombe, D., Van-Gils, J., Fergelot, P. *et al.* (2020) Evaluation of DNA methylation Episignatures for diagnosis and phenotype correlations in 42 Mendelian neurodevelopmental disorders. *Am. J. Hum. Genet.*, **106**, 356–370.
37. Greenwood Genetic Center (2020) *EpiSign Complete*. Greenwood Genetic Center, Greenwood, SC, https://www.ggc.org/test-finder-item/episign-complete.
38. Duffy, K.A., Cielo, C.M., Cohen, J.L., Gonzalez-Gandolfi, C.X., Griff, J.R., Hathaway, E.R., Kupa, J., Taylor, J.A., Wang, K.H., Ganguly, A. *et al.* (2019) Characterization of the Beckwith-Wiedemann spectrum: diagnosis and management. *Am. J. Med. Genet. C Semin. Med. Genet.*, **181**, 693–708.
39. Baker, S.W., Duffy, K.A., Richards-Yutz, J. and Kalish, J.M. (2020) Improved molecular detection of mosaicism in Beckwith-Wiedemann syndrome. *J. Med. Genet.*. doi: 10.1136/jmedgenet-2019-106498.
40. Cattanach, B. and Rasberry, C. (1993) Evidence of imprinting involving the distal region of mouse chromosome 12. *Mouse Genome*, **91**, 851–853.
41. Schmidt, J.V., Matteson, P.G., Jones, B.K., Guan, X.J. and Tilghman, S.M. (2000) The Dlk1 and Gtl2 genes are linked and reciprocally imprinted. *Genes Dev.*, **14**, 1997–2002.
42. Miyoshi, N., Wagatsuma, H., Wakana, S., Shiroishi, T., Nomura, M., Aisaka, K., Kohda, T., Surani, M.A., Kaneko-Ishino, T. and Ishino, F. (2000) Identification of an imprinted gene, Meg3/Gtl2 and its human homologue MEG3, first mapped on mouse distal chromosome 12 and human chromosome 14q. *Genes Cells*, **5**, 211–220.
43. Takada, S., Tevendale, M., Baker, J., Georgiades, P., Campbell, E., Freeman, T., Johnson, M.H., Paulsen, M. and Ferguson-Smith, A.C. (2000) Delta-like and Gtl2 are reciprocally expressed, differentially methylated linked imprinted genes on mouse chromosome 12. *Curr. Biol.*, **10**, 1135–1138.
44. Takada, S. (2002) Epigenetic analysis of the Dlk1-Gtl2 imprinted domain on mouse chromosome 12: implications for imprinting control from comparison with Igf2-H19. *Hum. Mol. Genet.*, **11**, 77–86.
45. Seitz, H., Youngson, N., Lin, S.-P., Dalbert, S., Paulsen, M., Bachellerie, J.-P., Ferguson-Smith, A.C. and Cavaillé, J. (2003) Imprinted microRNA genes transcribed antisense to a reciprocally imprinted retrotransposon-like gene. *Nat. Genet.*, **34**, 261–262.
46. Seitz, H., Royo, H., Bortolin, M.-L. *et al.* (2004) A large imprinted microRNA gene cluster at the mouse Dlk1-Gtl2 domain. *Genome Res.*, **14**, 1741–1748.
47. Cavaillé, J., Seitz, H., Paulsen, M., Lin, S.-P., Ferguson-Smith, A.C. and Cavaillé, J. (2002) Identification of tandemly-repeated C/D snoRNA genes at the imprinted human 14q32 domain reminiscent of those at the Prader–Willi/Angelman syndrome region. *Hum. Mol. Genet.*, **11**, 1527–1538.
48. Tsai, C.-E., Lin, S.-P., Ito, M., Takagi, N., Takada, S. and Ferguson-Smith, A.C. (2002) Genomic imprinting contributes to thyroid hormone metabolism in the mouse embryo. *Curr. Biol.*, **12**, 1221–1226.
49. Paulsen, M., Takada, S., Youngson, N.A., Benchaib, M., Charlier, C., Segers, K., Georges, M. and Ferguson-Smith, A.C. (2001) Comparative sequence analysis of the imprinted Dlk1–Gtl2 locus in three mammalian species reveals highly conserved genomic elements and refines comparison with the Igf2–H19 region. *Genome Res.*, **11**, 2085–2094.
50. Georgiades, P., Watkins, M., Surani, M.A. and Ferguson-Smith, A.C. (2000) Parental origin-specific developmental defects in mice with uniparental disomy for chromosome 12. *Development*, **127**, 4719–4728.
51. Sutton, V.R., McAlister, W.H., Bertin, T.K., Kaffe, S., Wang, J.-C.C., Yano, S., Shaffer, L.G., Lee, B., Epstein, C.J. and Villar, A.J. (2003) Skeletal defects in paternal uniparental disomy for chromosome 14 are re-capitulated in the mouse model (paternal uniparental disomy 12). *Hum. Genet.*, **113**, 447–451.
52. Tevendale, M., Watkins, M., Rasberry, C., Cattanach, B. and Ferguson-Smith, A.C. (2006) Analysis of mouse conceptuses with uniparental duplication/deficiency for distal chromosome 12: comparison with chromosome 12 uniparental disomy and implications for genomic imprinting. *Cytogenet. Genome Res.*, **113**, 215–222.
53. Kumamoto, S., Takahashi, N., Nomura, K., Fujiwara, M., Kijioka, M., Uno, Y., Matsuda, Y., Sotomaru, Y. and Kono, T. (2017) Overexpression of microRNAs from the Gtl2-Rian locus contributes to postnatal death in mice. *Hum. Mol. Genet.*, **26**, 3653–3662.
54. Lin, S.-P., Coan, P., da Rocha, S.T., Seitz, H., Cavaille, J., Teng, P.-W., Takada, S. and Ferguson-Smith, A.C. (2007) Differential regulation of imprinting in the murine embryo and placenta by the Dlk1-Dio3 imprinting control region. *Development*, **134**, 417–426.
55. Lin, S.-P., Youngson, N., Takada, S., Seitz, H., Reik, W., Paulsen, M., Cavaille, J. and Ferguson-Smith, A.C. (2003) Asymmetric regulation of imprinting on the maternal and paternal chromosomes at the Dlk1-Gtl2 imprinted cluster on mouse chromosome 12. *Nat. Genet.*, **35**, 97–102.
56. Saito, T., Hara, S., Kato, T., Tamano, M., Muramatsu, A., Asahara, H. and Takada, S. (2018) A tandem repeat array in IG-DMR is essential for imprinting of paternal allele at the Dlk1–Dio3 domain during embryonic development. *Hum. Mol. Genet.*, **27**, 3283.
57. Hosoki, K., Ogata, T., Kagami, M., Tanaka, T. and Saitoh, S. (2008) Epimutation (hypomethylation) affecting the chromosome 14q32.2 imprinted region in a girl with upd(14)mat-like phenotype. *Eur. J. Hum. Genet.*, **16**, 1019.
58. Briggs, T.A., Lokulo-Sodipe, K., Chandler, K.E., Mackay, D.J.G. and Temple, I.K. (2016) Temple syndrome as a result of isolated hypomethylation of the 14q32 imprinted DLK1/MEG3 region. *Am. J. Med. Genet. A*, **170**, 170–175.

59. Nowak, K., Stein, G., Powell, E., He, L.M., Naik, S., Morris, J., Marlow, S. and Davis, T.L. (2011) Establishment of paternal allele-specific DNA methylation at the imprinted mouse Gtl2 locus. *Epigenetics*, **6**, 1012–1020.
60. Takahashi, N., Okamoto, A., Kobayashi, R., Shirai, M., Obata, Y., Ogawa, H., Sotomaru, Y. and Kono, T. (2009) Deletion of Gtl2 , imprinted non-coding RNA, with its differentially methylated region induces lethal parent-origin-dependent defects in mice. *Hum. Mol. Genet.*, **18**, 1879–1888.
61. Zhou, Y., Cheunsuchon, P., Nakayama, Y., Lawlor, M.W., Zhong, Y., Rice, K.A., Zhang, L., Zhang, X., Gordon, F.E., Lidov, H.G.W. *et al.* (2010) Activation of paternally expressed genes and perinatal death caused by deletion of the Gtl2 gene. *Development*, **137**, 2643–2652.
62. Schuster-Gossler, K., Simon-Chazottes, D., Guénet, J.-L., Zachgo, J. and Gossler, A. (1996) Gtl2lacZ, an insertional mutation on mouse chromosome 12 with parental origin-dependent phenotype. *Mamm. Genome*, **7**, 20–24.
63. Steshina, E.Y., Carr, M.S., Glick, E.A., Yevtodiyenko, A., Appelbe, O.K. and Schmidt, J.V. (2006) Loss of imprinting at the Dlk1 - Gtl2 locus caused by insertional mutagenesis in the Gtl2 5' region. *BMC Genet.*, **7**, 1–21.
64. Charalambous, M., da Rocha, S.T., Hernandez, A. and Ferguson-Smith, A.C. (2014) Perturbations to the IGF1 growth pathway and adult energy homeostasis following disruption of mouse chromosome 12 imprinting. *Acta Physiol.*, **210**, 174–187.
65. Ogata, T. and Kagami, M. (2016) Kagami–Ogata syndrome: a clinically recognizable upd(14)pat and related disorder affecting the chromosome 14q32.2 imprinted region. *J. Hum. Genet.*, **61**, 87–94.
66. Sekita, Y., Wagatsuma, H., Nakamura, K., Ono, R., Kagami, M., Wakisaka, N., Hino, T., Suzuki-Migishima, R., Kohda, T. and Ogura, A. (2008) Role of retrotransposon-derived imprinted gene, Rtl1, in the feto-maternal interface of mouse placenta. *Nat. Genet.*, **40**, 243–248.
67. Ito, M., Sferruzzi-Perri, A.N., Edwards, C.A., Adalsteinsson, B.T., Allen, S.E., Loo, T.-H., Kitazawa, M., Kaneko-Ishino, T., Ishino, F., Stewart, C.L. and Ferguson-Smith, A.C. (2015) A trans-homologue interaction between reciprocally imprinted miR-127 and Rtl1 regulates placenta development. *Development*, **142**, 2425–2430.
68. Labialle, S., Marty, V., Bortolin-Cavaillé, M.-L., Hoareau-Osman, M., Pradère, J.-P., Valet, P., Martin, P.G.P. and Cavaillé, J. (2014) The miR-379/miR-410 cluster at the imprinted Dlk1-Dio3 domain controls neonatal metabolic adaptation. *EMBO J.*, **33**, 2216–2230.
69. Dauber, A., Cunha-Silva, M., Macedo, D.B., Brito, V.N., Abreu, A.P., Roberts, S.A., Montenegro, L.R., Andrew, M., Kirby, A., Weirauch, M.T. *et al.* (2017) Paternally inherited DLK1 deletion associated with familial central precocious puberty. *J. Clin. Endocrinol. Metab.*, **102**, 1557–1567.
70. Macedo, D.B. and Kaiser, U.B. (2019) DLK1, notch signaling and the timing of puberty. *Semin. Reprod. Med.*, **37**, 174–181.
71. Moon, Y.S., Smas, C.M., Lee, K., Villena, J.A., Kim, K.-H., Yun, E.J. and Sul, H.S. (2002) Mice lacking paternally expressed Pref-1/Dlk1 display growth retardation and accelerated adiposity. *Mol. Cell. Biol.*, **22**, 5585–5592.
72. Court, F., Tayama, C., Romanelli, V., Martin-Trujillo, A., Iglesias-Platas, I., Okamura, K., Sugahara, N., Simón, C., Moore, H., Harness, J.V. *et al.* (2014) Genome-wide parent-of-origin DNA methylation analysis reveals the intricacies of human imprinting and suggests a germline methylation-independent mechanism of establishment. *Genome Res.*, **24**, 554–569.
73. Benetatos, L., Hatzimichael, E., Londin, E., Vartholomatos, G., Loher, P., Rigoutsos, I. and Briasoulis, E. (2013) The microRNAs within the DLK1-DIO3 genomic region: involvement in disease pathogenesis. *Cell. Mol. Life Sci.*, **70**, 795–814.
74. Hernandez, A., Martinez, M.E., Croteau, W. and St Germain, D.L. (2004) Complex organization and structure of sense and antisense transcripts expressed from the DIO3 gene imprinted locus. *Genomics*, **83**, 413–424.
75. Mackay, D.J.G. and Temple, I.K. (2017) Human imprinting disorders: principles, practice, problems and progress. *Eur. J. Med. Genet.*, **60**, 618–626.
76. Llères, D., Moindrot, B., Pathak, R., Piras, V., Matelot, M., Pignard, B., Marchand, A., Poncelet, M., Perrin, A., Tellier, V. *et al.* (2019) CTCF modulates allele-specific sub-TAD organization and imprinted gene activity at the mouse Dlk1-Dio3 and Igf2-H19 domains. *Genome Biol.*, **20**, 272.
77. Martinez, M.E., Cox, D.F., Youth, B.P. and Hernandez, A. (2016) Genomic imprinting of DIO3, a candidate gene for the syndrome associated with human uniparental disomy of chromosome 14. *Eur. J. Hum. Genet.*, **24**, 1617–1621.
78. Hernandez, A. and Stohn, J.P. (2018) The type 3 deiodinase: epigenetic control of brain thyroid hormone action and neurological function. *Int. J. Mol. Sci.*, **19**, 1804.
79. Gordon, F.E., Nutt, C.L., Cheunsuchon, P., Nakayama, Y., Provencher, K.A., Rice, K.A., Zhou, Y., Zhang, X. and Klibanski, A. (2010) Increased expression of angiogenic genes in the brains of mouse meg3-null embryos. *Endocrinology*, **151**, 2443–2452.
80. Charlier, C., Segers, K., Wagenaar, D., Karim, L., Berghmans, S., Jaillon, O., Shay, T., Weissenbach, J., Cockett, N., Gyapay, G. and Georges, M. (2001) Human-ovine comparative sequencing of a 250-kb imprinted domain encompassing the callipyge (clpg) locus and identification of six imprinted transcripts: DLK1, DAT, GTL2, PEG11, antiPEG11, and MEG8. *Genome Res.*, **11**, 850–862.
81. Davis, E., Caiment, F., Tordoir, X., Cavaillé, J., Ferguson-Smith, A., Cockett, N., Georges, M. and Charlier, C. (2005) RNAi-mediated allelic trans-interaction at the imprinted Rtl1/Peg11 locus. *Curr. Biol.*, **15**, 743–749.
82. Goossens, E.A.C., de Vries, M.R., Simons, K.H., Putter, H., Quax, P.H.A. and Nossent, A.Y. (2019) miRMap: profiling 14q32 microRNA expression and DNA methylation throughout the human vasculature. *Front. Cardiovasc. Med.*, **6**, 113.
83. Kameswaran, V., Bramswig, N.C., McKenna, L.B., Penn, M., Schug, J., Hand, N.J., Chen, Y., Choi, I., Vourekas, A., Won, K.-J. *et al.* (2014) Epigenetic regulation of the DLK1-MEG3 microRNA cluster in human type 2 diabetic islets. *Cell Metab.*, **19**, 135–145.
84. Håkansson, K.E.J., Goossens, E.A.C., Trompet, S., van Ingen, E., R de Vries, M., V C T van der Kwast, R., Ripa, R.S., Kastrup, J., Hohensinner, P.J., Kaun, C. *et al.* (2019) Genetic associations and regulation of expression indicate an independent role for 14q32 snoRNAs in human cardiovascular disease. *Cardiovasc. Res.*, **115**, 1519–1532.
85. Wang, Y., Zhao, L., Smas, C., Sul, H.S. (2010) Pref-1 interacts with Fibronectin to inhibit adipocyte differentiation. *Mol Cell Biol*, **30**, 3480–3492.